Parameterization of Turbulent Diffusivity in the Deep Ocean

Group Representative
Toshiyuki Hibiya   Graduate School of Science, The University of Tokyo

Authors
Yoshihiro Niwa   Graduate School of Science, The University of Tokyo
Toshiyuki Hibiya   Graduate School of Science, The University of Tokyo

The East China Sea and the adjacent seas are one of the most significant generation regions of the M_2 internal tide and, hence the associated turbulent mixing in the world's oceans. In the present study, we investigate the distribution and energetics of the M_2 internal tide around the continental shelf edge in the East China Sea using a three-dimensional numerical model. The numerical experiment shows that M_2 internal tides are effectively generated over prominent topographic features such as the subsurface ridges in the Bashi/Luzon and Tokara Straits, the ridges along the Ryukyu Island chain, and the continental shelf slope in the East China Sea, the former particularly so. The conversion rate from M_2 barotropic to baroclinic energy over the whole model domain is estimated to be 35 GW. It is, however, found that about half of the excited M_2 internal tidal energy is dissipated before radiating into the open ocean, suggesting the presence of intense turbulent mixing in close proximity to the generation sites.

Keywords: Internal tide, Turbulent diffusivity, Internal gravity wave, Thermohaline circulation

1. Introduction

It is widely recognized that internal tides have strong influence on the global thermohaline circulation, because it contribute significantly to deep ocean mixing, the essential process for the maintenance of the thermohaline circulation [*Munk and Wunsch*, 1998]. Internal tides generated by strong tide-topography interactions occasionally break causing intense turbulent mixing [*Lien and Gregg*, 2001]. Turbulent mixing may also be induced far from wave generation sites, because propagating internal tides can nonlinearly interact with the background internal waves and cascade part of their energy down to small scales where breaking can occur.

The East China Sea and adjacent seas are one of the most important generation regions of internal tides, and hence the associated turbulent mixing. Indeed, using a two-dimensional analytical model, *Baines* [1982] predicted that the continental shelf slope in the East China Sea is the second largest generator of the M_2 internal tide among the major continental shelf slopes in the world's oceans. Vigorous mixing, the strength of which depends on the phase of the semidiurnal tidal current, has been observed in the East China Sea [*Matsuno et al.*, 1994]. The East China Sea and adjacent seas are thus interesting regions for the study of internal tides and turbulent mixing. In the present study, we numerically investigate the spatial distribution of the M_2 internal tide and its energetics in the East China Sea and adjacent seas using a
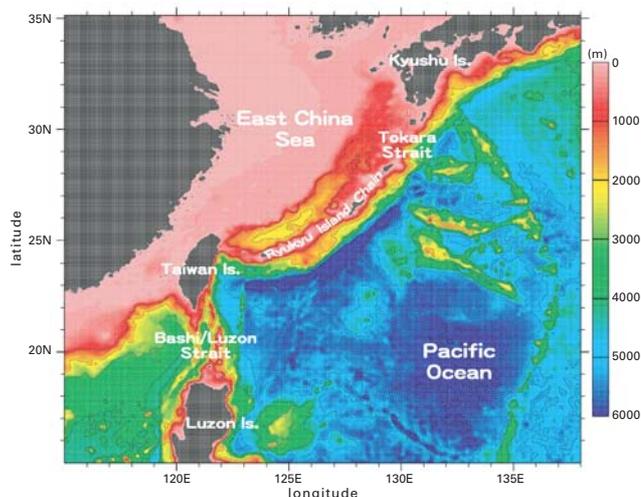
Fig. 1 Bathymetry in the model domain.

high-resolution, three-dimensional model that takes into account realistic tidal forcing as well as realistic bathymetry.

2. Numerical experiment

Figure 1 shows the bathymetry of the model domain which includes a prominent ridge running from the south of Kyushu Island through the Ryukyu Island chain and across the Bashi/Luzon Strait to Luzon Island, and the continental shelf slope in the East China Sea that runs parallel to this ridge.

The numerical simulation was carried out using the Princeton Ocean Model [*Blumberg and Mellor*, 1987], which

solves the three-dimensional, free-surface primitive equations under the hydrostatic and Boussinesq approximations in the terrain following sigma coordinate system. The horizontal grid spacing is set to be 1/32° both in the longitudinal and latitudinal directions, and there are 50 sigma levels in the vertical.

The model topography was determined from the bathymetric data of *Smith and Sandwell* [1997], and the background basic temperature and salinity were from each annual mean data of the World Ocean Atlas [*Levitus and Boyer*, 1994; *Levitus et al.*, 1994]. The model was forced at the open boundary by prescribing the M_2 surface tide through a forced gravity wave radiation condition as employed in *Niwa and Hibiya* [2001]. The amplitude of the M_2 surface tide at the open boundary was specified by using the global
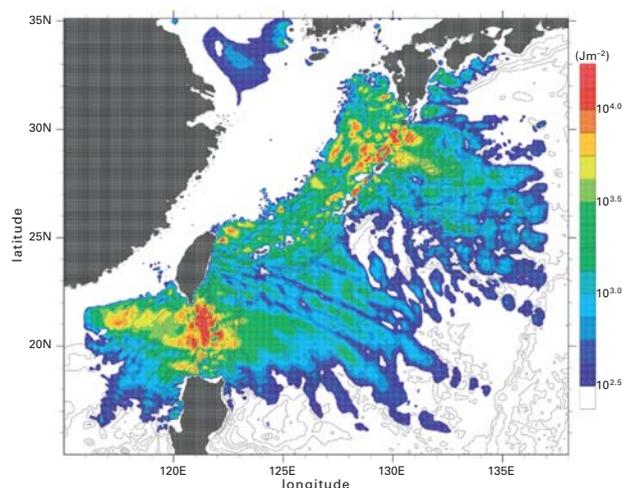
Fig. 2 Model-predicted distribution of the depth-integrated kinetic energy of the M_2 internal tide averaged over the final 2 days of the calculation. The background contours show the bathymetry (contour interval is 1000 m).
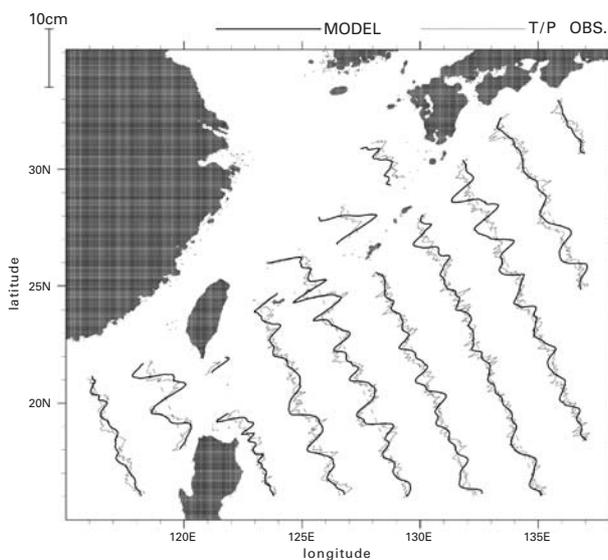
Fig. 3 High-pass filtered amplitude of the M_2 tidal surface elevation along Topex/Poseidon descending ground tracks obtained from the model prediction (thick solid lines) and Topex/Poseidon altimeter observations (thin solid lines).

tide model of *Matsumoto et al.* [2000].

The model was driven for 15 days from an initial state of rest with time steps of 90 s and 3 s for the baroclinic and barotropic tides, respectively. The calculated time series for the final 2 days were harmonically analyzed to obtain the amplitude and phase of the M_2 surface and internal tidal responses.

3. Results

Figure 2 shows the distribution of the depth-integrated kinetic energy of the M_2 internal tide. We can see that the M_2 internal tide is effectively generated over prominent topographic features such as the subsurface ridges in the Bashi/Luzon and Tokara Straits, the ridges along the Ryukyu Island chain, and the continental shelf slope in the East China Sea, the former particularly so. These topographic features are characterized by steep slopes at the depth of the thermocline onto which the M_2 surface tide is incident almost normally.

The M_2 internal tides propagating away from the above mentioned multiple source regions interfere each other to create complex wave pattern in the western North Pacific. Figure 3 shows the short-wavelength surface elevation amplitude fluctuations along Topex/Poseidon ground tracks obtained from the numerical experiment (thick solid lines) and from Topex/Poseidon altimeter observations (thin solid lines). We can see that the magnitude and wavelength of the model predicted surface fluctuations are in general agreement with Topex/Poseidon altimeter observations, indicating the validity of the present numerical simulation.

To investigate the generation of the M_2 internal tide more in detail, we demonstrate in Figure 4 the distribution of the depth-integrated energy conversion rate from the M_2 barotropic to baroclinic tide. The M_2 baroclinic conversion rate integrated over the whole model domain amounts to 35 GW, which corresponds to about 5% of the global conversion rate of the M_2 tide estimated by *Egbert and Ray* [2000] and about 1.5% of the power required to maintain the global thermohaline circulation [*Munk and Wunsch*, 1998]. Figure 4 shows that the largest M_2 baroclinic energy was generated over the subsurface ridges in the Bashi/Luzon Strait where the net baroclinic energy conversion reaches 14 GW about 40% of the total baroclinic energy conversion over the whole model domain.

The red-colored numbers and arrows shown in Figure 4 indicate the value and direction of the M_2 barotropic energy flux across each section, respectively. The net M_2 barotropic energy flux onto the subsurface ridges in the Bashi/Luzon Strait is 56 GW, 25% of which (14 GW) is converted to M_2 baroclinic energy. After passing through the strait, the barotropic energy flux decreases to 41 GW, indicating 15 GW of the barotropic energy is lost within the Bashi/Luzon Strait which almost balances the conversion of barotropic to baroclinic energy.
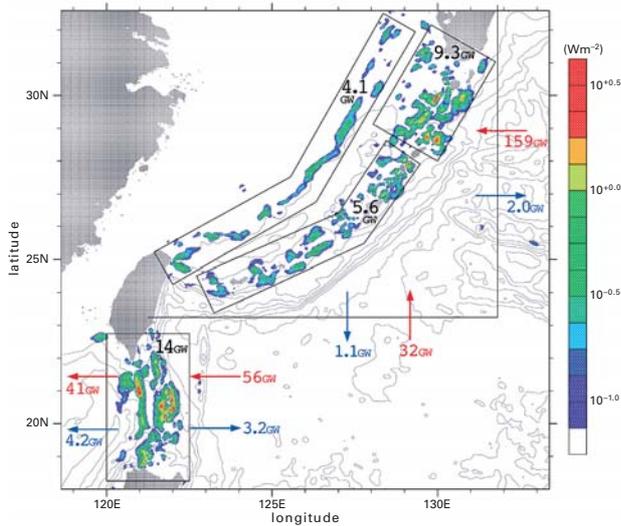
Fig. 4 Model-predicted distribution of the depth-integrated conversion rate from the M_2 barotropic to baroclinic tidal energy (shown by the color shading). The background contours show the bathymetry (contour interval is 1000m). The black-colored numbers indicate the conversion rate integrated over the area including each prominent topographic feature. The red-colored numbers and arrows indicate the value and direction of the M_2 barotropic energy flux across each section, whereas the blue-colored numbers and arrows indicate the value and direction of the M_2 baroclinic energy flux across each section.

The integrated M_2 baroclinic energy flux across each section is shown by the blue-colored numbers and arrows in Figure 4. It should be noted that the integrated baroclinic energy flux becomes much less than the net baroclinic energy conversion estimated over the prominent topographic features, indicating that considerable fraction of the excited baroclinic energy is dissipated before radiating away from each area.

In order to quantify the distribution of baroclinic energy

dissipation within the Bashi/Luzon Strait, we show in Figure 5 the spatial distributions of the (a) the baroclinic energy conversion, (b) the baroclinic energy flux divergence, and (c) the difference between (a) and (b). Significant difference between the baroclinic energy conversion rate and the baroclinic energy flux divergence can be found at the location of strong baroclinic energy conversion. This indicates that generated internal tides are subject to strong local dissipation in proximity to their generation sites. The local dissipation within the Bashi/Luzon Strait amounts to 5.2 GW corresponding to about 40% of the baroclinic energy generated in this region.

4. Summary and discussion

It is widely recognized that the internal tides play an important role in the maintenance of the thermohaline circulation by providing energy for deep ocean mixing. In the present study, we have investigated the distribution and energetics of the M_2 internal tides generated in the East China Sea and adjacent seas using a three-dimensional, primitive equation model that takes into account realistic tidal forcing as well as realistic bathymetry.

The most energetic M_2 internal tides have been found in the Bashi/Luzon Strait and the Tokara Strait where steep slopes onto which the M_2 surface tide is almost normally incident exist at the depth of the thermocline. It has been, however, found that nearly half of the excited baroclinic tidal energy is dissipated before radiating into the open ocean, which suggests the presence of intense turbulent mixing in close proximity to the generation sites.

The additional sensitivity experiments demonstrate that, as compared to the baroclinic conversion rate, the baroclinic dissipation rate is more dependent on the resolution of the bottom topography. This suggests that the local baroclinic
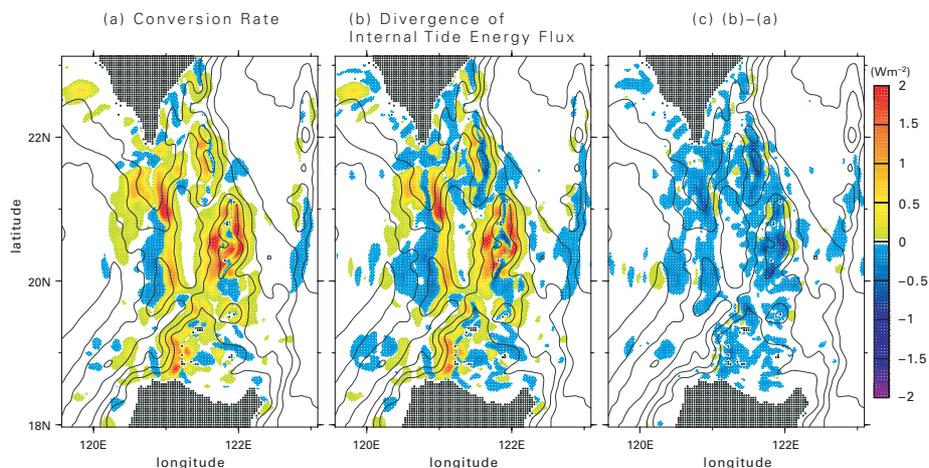
Fig. 5 Model predicted distribution of (a) the depth-integrated conversion rate from the M_2 barotropic to baroclinic tidal energy, (b) the divergence of the depth-integrated M_2 baroclinic energy flux, and (c) the difference between them (the baroclinic energy flux divergence minus the baroclinic conversion rate) in the Bashi/Luzon Strait (shown by the color shading). The background contours show the bathymetry (contour interval is 1000 m).

dissipation is caused by shear and/or advective instability of small-scale internal waves generated and/or scattered at the bottom topography. Nevertheless, the detailed mechanism for this strong local dissipation must await future investigation.

References

P. G. Baines, "On internal tide generation models", Deep-Sea Res., vol.29, pp.307–338, 1982.

A. F. Blumberg, and G. L. Mellor, "A description of a three-dimensional coastal ocean circulation model", Three-Dimensional Coastal Ocean Models, American Geophysical Union, pp.1–16, 1987.

G. D. Egbert, and R. D. Ray, "Significant Dissipation of Tidal Energy in the Deep Ocean Inferred From Satellite Altimeter Data, Nature, vol.405, pp.775–778, 2000.

S. Levitus, and T. P. Boyer, World Ocean Atlas 1994, Vol. 4, Temperature: NOAA Atlas NESDIS 4, U.S. Dep. of Commer., 1994.

S. Levitus, and R. Burgett and T. P. Boyer, World Ocean Atlas 1994, Vol.3, Salinity: NOAA Atlas NESDIS 3, U. S. Dep. of Commer., 1994.

R.-C. Lien, and M. C. Gregg, "Observation of turbulence in a tidal beam and across a coastal ridge", J. Geophys. Res., vol.106, pp.4575–4591, 2000.

K. Matsumoto, T. Takanezawa and M. Ooe, "Ocean tide models developed by assimilating Topex/Poseidon altimeter data into hydrodynamical model: a global model and a regional model around Japan", J. Oceanogr., vol.56, pp.567–581, 2000.

T. Matsuno, S. Kanari, and C. Kobayashi, and T. Hibiya, "Vertical mixing in the bottom mixed layer near the continental shelf break in the East China Sea", J. Oceanogr., vol.50, pp.437–448, 1994.

W. H. Munk, and C. Wunsch, "Abyssal recipes II: energetics of tidal and wind mixing", Deep-Sea Res., vol.45, pp.1977–2000, 1998.

Y. Niwa, and T. Hibiya, "Numerical study of the spatial distribution of the M_2 internal tide in the Pacific Ocean", J. Geophys. Res., vol.106, pp.22441–22449, 2001.

W. H. F. Smith, and D. T. Sandwell, "Global sea floor topography from satellite altimetry and ship depth soundings", Science, vol.277, pp.1956–1962, 1997.